Progress In Electromagnetics Research C, Vol. 42, 13–28, 2013

QUASI-ELLIPTIC WIDEBAND BANDPASS FILTERS USING STUBS LOADED ANTI-PARALLEL COUPLED-LINE

Jin Xu* **and Wen Wu**

Ministerial Key Laboratory of JGMT, Nanjing University of Science and Technology, Nanjing 210094, China

Abstract—This paper presents a new type of wideband bandpass filter (BPF) with quasi-elliptic frequency response by using proposed stubs loaded anti-parallel coupled-line. With different loads, the proposed stubs loaded anti-parallel coupled-line has different numbers of transmission zeros (TZs). These TZs are symmetrical along the designing frequency f_0. By using a quarter-wavelength parallel coupled-line to connect two proposed stubs loaded anti-parallel coupled-line, three wideband BPFs centered at $f_0 = 1.575\,\text{GHz}$ with quasi-elliptic frequency response are successfully designed. Good agreements between the simulations and measurements can be observed. The measured results also exhibits that the fabricated BPFs have the merits of low in-band insertion loss, good in-band return loss, sharp passband selectivity and high out-of-band rejection.

1. INTRODUCTION

Coupled-line is an usual and classical structure to exploit lowpass filter [1], bandstop filter [2–4], bandpass filter (BPF) [5–12], reconfigurable BPF [13] and dual-band BPF [14–17]. Although the lowpass, bandstop, reconfigurable and dual-band filters with coupled-line have good electrical performance, they often suffer from large circuit size due to the required quarter-wavelength or half-wavelength couple-line. Since the coupled-line can be equivalent to a susceptance inverter which is useful in BPF design, the coupled-line is much more widely used in single-band BPF design.

For conventional parallel coupled-line BPF, passband selectivity is determined by filter order. If a higher selectivity performance is

Received 17 June 2013, Accepted 6 July 2013, Scheduled 15 July 2013

* Corresponding author: Jin Xu (xujin2njust@126.com).

required, filter order must be increased, which leads to large circuit size. Moreover, the conventional parallel coupled-line BPF always suffers from second harmonic frequency. In order to overcome such a problem, many methods have been used to improve the coupled-line for generating new useful properties. In [5], terminated parallel coupled-line with different terminations was studied, and the designed BPF achieved second spurious-response suppression successfully. However, the claimed transmission zeros (TZs) could not be observed in the simulation and measured results, so that the filter did not have sharp passband. In [6, 7], grounded parallel coupled-line with shunt capacitors or series inductors were studied, and the designed BPFs had the merits of reduced circuit size and wide upper stopband. However, the lumped-element elements were used at microwave frequency, which increased the design procedure. In addition, the reported BPFs suffered from larger insertion losses than the conventional ones. In [8], the defected ground structures were etched underneath the input/output ports of a symmetrical parallel coupled-line BPF, so as to extend the stopband performance. However, the etched ground plane increased the installation complexity. In [9], the dual-mode open stub loaded parallel coupled-line with one TZ was proposed, and the TZ could be located at either lower side band or upper side band. By cascading two types of proposed dual-mode open stub loaded parallel coupled-line, a BPF with quasi-elliptic frequency response was reported. In [10], a coupled-line BPF with multiple capacitive cross-couplings to create four TZs was reported. Although it exhibited the quasi-elliptic frequency response, the BPF in [10] suffered from relatively large insertion loss. In [11], a good performance millimeter-wave BPF with two TZs was designed by using LTCC technique. In [12], a good performance BPF with quasi-elliptic frequency response was designed by using open stub loaded anti-parallel coupled-line. However, its 20 dB out-of-band rejection could not meet some high requirement application.

In general, most of these reported coupled-line BPFs have less than 10% fractional bandwidth (FBW). This paper presents a novel type of stubs loaded anti-parallel coupled-line. With different loads, the proposed stubs loaded anti-parallel coupled-line has two or four tunable TZs. By using a quarter-wavelength coupled-line to connect two same type of stubs loaded anti-parallel coupled-line together, a BPF with quasi-elliptic frequency response can be designed. As examples, three BPFs centered at 1.575 GHz are designed and fabricated. Detailed design procedure as well as simulated and measured results are discussed in the following sections.

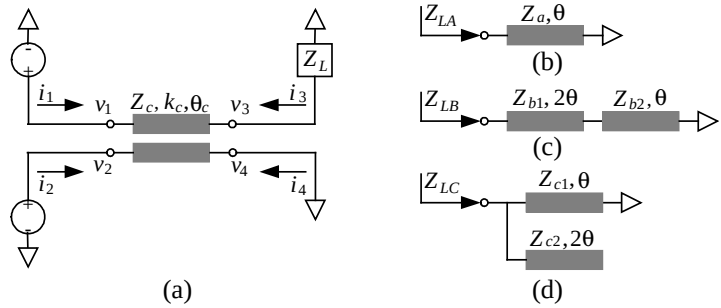

Figure 1. (a) Schematic of proposed stubs loaded anti-parallel coupled-line. (b) Load A. (c) Load B. (d) Load C.

2. ANALYSIS OF PROPOSED STUBS LOADED ANTI-PARALLEL COUPLED-LINE

2.1. *ABCD* Parameters of Stubs Loaded Anti-parallel Coupled-line

Figure 1(a) shows the schematic of proposed stubs loaded anti-parallel coupled-line with short-circuited port 4 and port 3 terminated by the load Z_L. In order to derive its two port $ABCD$ parameters, symmetric and anti-symmetric excitations of the ports are considered. According to the discussion in the Ref. [18], the following two equations can be obtained:

$$\begin{bmatrix} v_1 - v_2 \\ i_1 - i_2 \end{bmatrix} = \begin{bmatrix} \cos\theta_{co} & jZ_{co}\sin\theta_{co} \\ jY_{co}\sin\theta_{co} & \cos\theta_{co} \end{bmatrix} \begin{bmatrix} v_4 - v_3 \\ -(i_4 - i_3) \end{bmatrix} \tag{1a}$$

$$\begin{bmatrix} v_1 + v_2 \\ i_1 + i_2 \end{bmatrix} = \begin{bmatrix} \cos\theta_{ce} & jZ_{ce}\sin\theta_{ce} \\ jY_{ce}\sin\theta_{ce} & \cos\theta_{ce} \end{bmatrix} \begin{bmatrix} v_4 + v_3 \\ -(i_4 + i_3) \end{bmatrix} \tag{1b}$$

where $\theta_{e,o}$ denote the even-/odd-mode electrical length of coupled-line, $Z_{ce} = Z_c[(1+k_c)/(1-k_c)]^{1/2}$ and $Z_{co} = Z_c[(1-k_c)/(1+k_c)]^{1/2}$. For discussion simplicity, $\theta_e = \theta_o = \theta = \pi/2$ at the designing frequency f_0 is considered in this paper. Since the boundary condition at port 3 and port 4 are $v_3 = -i_3 Z_L$ and $v_4 = 0$, its $ABCD$ parameters are solved as

$$\begin{bmatrix} v_1 \\ i_1 \end{bmatrix} = \begin{bmatrix} A_i & B_i \\ C_i & D_i \end{bmatrix} \begin{bmatrix} v_2 \\ -i_2 \end{bmatrix} = \begin{bmatrix} \frac{u_1}{u_5} & -\frac{u_3}{u_7} + \frac{u_1 u_6}{u_5 u_7} \\ \frac{u_2}{u_5} & -\frac{u_4}{u_7} + \frac{u_2 u_6}{u_5 u_7} \end{bmatrix} \begin{bmatrix} v_2 \\ -i_2 \end{bmatrix} \tag{2a}$$

$$\begin{bmatrix} v_2 \\ i_2 \end{bmatrix} = \begin{bmatrix} A_o & B_o \\ C_o & D_o \end{bmatrix} \begin{bmatrix} v_1 \\ -i_1 \end{bmatrix} = \frac{1}{u_1 u_4 - u_2 u_3} \begin{bmatrix} u_4 u_5 - u_2 u_6 & -u_1 u_6 + u_3 u_5 \\ -u_2 u_7 & -u_1 u_7 \end{bmatrix} \begin{bmatrix} v_1 \\ -i_1 \end{bmatrix} \tag{2b}$$

where $u_1 = -j[(Z_{ce} + Z_{co})\sin\theta]/2$, $u_2 = -\cos\theta$, $u_3 = j[(Z_{co} - Z_{ce})\sin\theta]/2$, $u_4 = j[(Y_{co} - Y_{ce})Z_L \sin\theta]/2$, $u_5 = -j[(Z_{co} - Z_{ce})\sin\theta]/2$, $u_6 = -Z_L\cos\theta - j[(Z_{ce} + Z_{co})\sin\theta]/2$ and $u_7 = -\cos\theta - j[(Y_{co} + Y_{ce})Z_L \sin\theta]/2$.

2.2. Transmission Zeros (TZs) of Stubs Loaded Anti-parallel Coupled-line

The TZs of the above stubs loaded anti-parallel coupled-line is determined by $A_{i,o}D_{i,o} = B_{i,o}C_{i,o}$. After simplification, the TZs are then

$$u_1 u_4 = u_2 u_3 \tag{3}$$

Three types of loads, i.e., Loads A, B and C as shown in Figures 1(b)∼(d), are investigated in this paper, where $Z_{LA} = jZ_a \tan\theta$, $Z_{LB} = jZ_{b1}(Z_{b1}\tan 2\theta + Z_{b2}\tan\theta)/(Z_{b1} - Z_{b2}\tan\theta\tan 2\theta)$ and $Z_{LC} = jZ_{c1}Z_{c2}\tan\theta\cot 2\theta/(Z_{c2}\cot 2\theta - Z_{c1}\tan\theta)$. Thus, the TZs of anti-parallel coupled line with Load A are determined by

$$\tan^2\theta = \frac{2Z_{ce}Z_{co}}{Z_a(Z_{ce} + Z_{co})} = \frac{Z_c\sqrt{1-k_c^2}}{Z_a} \tag{4}$$

Equation (4) have two real roots within the frequency range $[0,\ 2f_0]$, which are given as

$$f_{Az1} = \frac{2f_0}{\pi}\arctan\sqrt{\frac{Z_c\sqrt{1-k_c^2}}{Z_a}} \tag{5a}$$

$$f_{Az2} = \frac{2f_0}{\pi}\left[\pi - \arctan\sqrt{\frac{Z_c\sqrt{1-k_c^2}}{Z_a}}\right] \tag{5b}$$

That is, the anti-parallel coupled line with Load A has two tunable TZs within the frequency range $[0,\ 2f_0]$. These two TZs have the relationship of $0 < f_{Az1} < f_0 < f_{Az2} < 2f_0$. The TZs of anti-parallel coupled line with Load B are determined by

$$A_B\tan^4\theta + B_B\tan^2\theta + C_B = 0 \tag{6}$$

where $A_B = 2Z_cZ_{b1}Z_{b2}/(1-k_c^2)^{1/2}$, $B_B = -[2Z_c(2Z_{b1}^2 + Z_{b1}Z_{b2})/(1-k_c^2)^{1/2} + 2Z_c^2(Z_{b1} + 2Z_{b2})]$ and $C_B = 2Z_c^2Z_{b1}$. Since $A_B > 0$, $B_B < 0$, $C_B > 0$ and $B_B^2 - 4A_BC_B > 0$ are always built, Equation (6) has four

real roots within the frequency range $[0,\ 2f_0]$, which can be expressed as

$$f_{Bz1} = \frac{2f_0}{\pi}\arctan\sqrt{\frac{-B_B-\sqrt{B_B^2-4A_BC_B}}{2A_B}} \tag{7a}$$

$$f_{Bz2} = \frac{2f_0}{\pi}\left[\pi-\arctan\sqrt{\frac{-B_B-\sqrt{B_B^2-4A_BC_B}}{2A_B}}\right] \tag{7b}$$

$$f_{Bz3} = \frac{2f_0}{\pi}\arctan\sqrt{\frac{-B_B+\sqrt{B_B^2-4A_BC_B}}{2A_B}} \tag{7c}$$

$$f_{Bz4} = \frac{2f_0}{\pi}\left[\pi-\arctan\sqrt{\frac{-B_B+\sqrt{B_B^2-4A_BC_B}}{2A_B}}\right] \tag{7d}$$

Thus, the anti-parallel coupled line with Load B has four tunable TZs within the frequency range $[0,\ 2f_0]$. These four TZs have the relationship of $0 < f_{Bz1} < f_{Bz3} < f_0 < f_{Bz4} < f_{Bz2} < 2f_0$. The TZs of anti-parallel coupled line with Load C are determined by

$$A_C\tan^4\theta + B_C\tan^2\theta + C_C = 0 \tag{8}$$

where $A_B = 2Z_cZ_{c1}Z_{c2}/(1-k_c^2)^{1/2}$, $B_B = -[2Z_cZ_{c1}Z_{c2}/(1-k_c^2)^{1/2} + 2Z_c^2(2Z_{c1}+Z_{b2})]$ and $C_B = 2Z_c^2Z_{c2}$. Since $A_c > 0$, $B_c < 0$, $C_c > 0$ and $B_c^2 - 4A_cC_c > 0$ are always built, Equation (8) also has four real roots within the frequency range $[0,\ 2f_0]$, which are derived as

$$f_{Cz1} = \frac{2f_0}{\pi}\arctan\sqrt{\frac{-B_C-\sqrt{B_C^2-4A_CC_C}}{2A_C}} \tag{9a}$$

$$f_{Cz2} = \frac{2f_0}{\pi}\left[\pi-\arctan\sqrt{\frac{-B_C-\sqrt{B_C^2-4A_CC_C}}{2A_C}}\right] \tag{9b}$$

$$f_{Cz3} = \frac{2f_0}{\pi}\arctan\sqrt{\frac{-B_C+\sqrt{B_C^2-4A_CC_C}}{2A_C}} \tag{9c}$$

$$f_{Cz4} = \frac{2f_0}{\pi}\left[\pi - \arctan\sqrt{\frac{-B_C + \sqrt{B_C^2 - 4A_C C_C}}{2A_C}}\right] \tag{9d}$$

Thus, the anti-parallel coupled line with Load C also has four tunable TZs within the frequency range $[0,\ 2f_0]$. These four TZs have the relationship of $0 < f_{Cz1} < f_{Cz3} < f_0 < f_{Cz4} < f_{Cz2} < 2f_0$.

The above TZs repeat periodically at every frequency range $(2nf_0,\ 2(n+1)f_0)$, where n is an integer. These TZs are symmetrical along f_0. In addition, the proposed stubs loaded anti-parallel coupled-line has two fixed TZs at 0 and $2f_0$.

3. ANALYSIS OF PROPOSED QUASI-ELLIPTIC WIDEBAND BANDPASS FILTERS (BPFS)

A two-end shorted quarter-wavelength parallel coupled-line is used to connect the above stubs loaded anti-parallel coupled line together for build up three-stage BPFs with quasi-elliptic frequency responses. The schematic of proposed BPFs is shown in Figure 2. The input/output stages are the proposed stubs loaded anti-parallel coupled-line and the middle stage is the classical two-end shorted parallel coupled-line. The $ABCD$ parameters of proposed three-stage BPF is given as

$$\begin{bmatrix} A & B \\ C & D \end{bmatrix} = \begin{bmatrix} A_i & B_i \\ C_i & D_i \end{bmatrix} \begin{bmatrix} A_p & B_p \\ C_p & D_p \end{bmatrix} \begin{bmatrix} A_o & B_o \\ C_o & D_o \end{bmatrix} \tag{10}$$

The $ABCD$ parameters of two-end shorted parallel coupled-line can be derived from the Ref. [5] as

$$\begin{bmatrix} A_p & B_p \\ C_p & D_p \end{bmatrix}$$

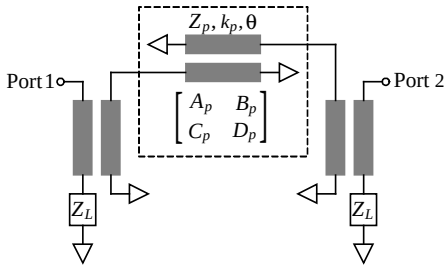

Figure 2. Three-stage BPF with quasi-elliptic frequency response.

$$= \frac{1}{j2Z_{pe}Z_{po}(Z_{pe}-Z_{po})\csc\theta} \begin{bmatrix} -j2Z_{pe}Z_{po}(Z_{pe}+Z_{po})\cot\theta & 4(Z_{pe}Z_{po})^2 \\ Z_{pe}^2+Z_{po}^2-2Z_{pe}Z_{po}(\csc^2\theta+\cot^2\theta) & -j2Z_{pe}Z_{po}(Z_{pe}+Z_{po})\cot\theta \end{bmatrix} \quad (11)$$

where $Z_{pe} = Z_p[(1+k_p)/(1-k_p)]^{1/2}$ and $Z_{po} = Z_p[(1-k_p)/(1+k_p)]^{1/2}$. The transmission and reflection coefficients of proposed BPF are determined by [19]

$$S_{11} = \frac{A+B/Z_0-CZ_0-D}{A+B/Z_0+CZ_0+D} \quad (12a)$$

$$S_{12} = \frac{2(AD-BC)}{A+B/Z_0+CZ_0+D} \quad (12b)$$

$$S_{21} = \frac{2}{A+B/Z_0+CZ_0+D} \quad (12c)$$

$$S_{22} = \frac{-A+B/Z_0-CZ_0+D}{A+B/Z_0+CZ_0+D} \quad (12d)$$

Since the proposed BPF structure is rotational symmetry, it has $S_{11} = S_{22}$ and $S_{21} = S_{22}$.

3.1. Filter *A*

For the BPF based on the anti-parallel coupled-line with Load A (named Filter A), $Z_a = 95\,\Omega$ is firstly pre-selected. Under $Z_p = 100\,\Omega$ and $k_p = 0.2$, Figure 3 plots the variation of TZs, -3 dB bandwidth (BW) and return loss (RL) versus different values of Z_c and k_c. It can

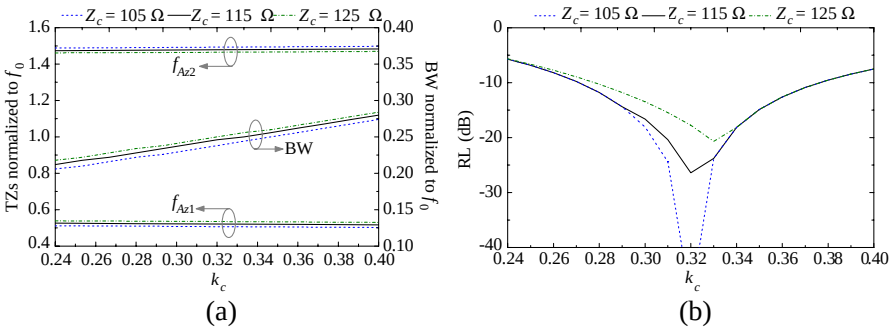

Figure 3. (a) Variation of TZs and BW versus Z_c and k_c. (b) Variation of RL versus Z_c and k_c.

be seen from Figure 3(a) that two TZs move close to f_0 as Z_c and k_c increase, while -3 dB BW increases as Z_c and k_c increase. Moreover, the TZs move close to f_0 very slowly as k_c increases, so that TZs can be mainly tuned by Z_c. It can be seen from Figure 3(b) that as k_c increases, the RL becomes better firstly and then becomes worse. A smaller value of Z_c leads to a better RL from $k_c = 0.28$ to $k_c = 0.34$. Under $Z_c = 115\,\Omega$ and $k_c = 0.31$, Figure 4 plots the variation of $|S_{21}|$ and $|S_{11}|$ versus different values of Z_p and k_p. It can be seen from Figure 4(a) that Z_p can be used to tune $|S_{11}|$ separately and has almost no effect on FBW. FBW of filter A can be tuned by k_c and k_p, as shown in Figure 3(a) and Figure 4(b).

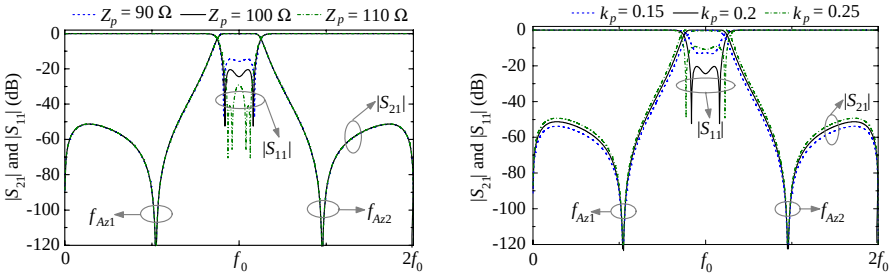

Figure 4. (a) Variation of $|S_{21}|$ and $|S_{11}|$ versus Z_p ($k_p = 0.2$ fixed). (b) Variation of $|S_{21}|$ and $|S_{11}|$ versus k_p ($Z_p = 100\,\Omega$ fixed).

3.2. Filter *B*

For the BPF based on the anti-parallel coupled-line with Load B (named Filter B), $Z_{b1} = 85\,\Omega$ is firstly pre-selected. Since k_c has a weak effect on the TZs and can be used to tune FBW as discussed in the above texts, $k_c = 0.3$ is also pre-selected. Under $Z_p = 100\,\Omega$ and $k_p = 0.18$, Figure 5 plots the variation of TZs, -3 dB BW and RL versus different values of $r_{bc} = Z_c/Z_{b1}$ and $r_{b12} = Z_{b2}/Z_{b1}$. As shown in Figure 5(a), the TZs of Filter B move apart from f_0 as r_{b12} increases, while r_{bc} has weak effect on TZs. It can be seen from Figure 5(b) that -3 dB BW of Filter B increases as r_{bc} increases, while -3 dB BW of Filter B almost keep constant as r_{b12} varies. Figure 5(b) also shows that RL of Filter B becomes better as r_{b12} increases, and a smaller value of r_{bc} leads to a better RL. Under $r_{bc} = 1.0$ and $r_{b12} = 1.65$, Figure 6 plots the variation of $|S_{21}|$ and $|S_{11}|$ versus different values of Z_p and k_p. It can be seen from Figure 6(a) that Z_p can be used to tune $|S_{11}|$ separately and has almost no effect on BW. -3 dB BW of Filter B can be slightly tuned by k_p. Thus, -3 dB FBW of Filter B

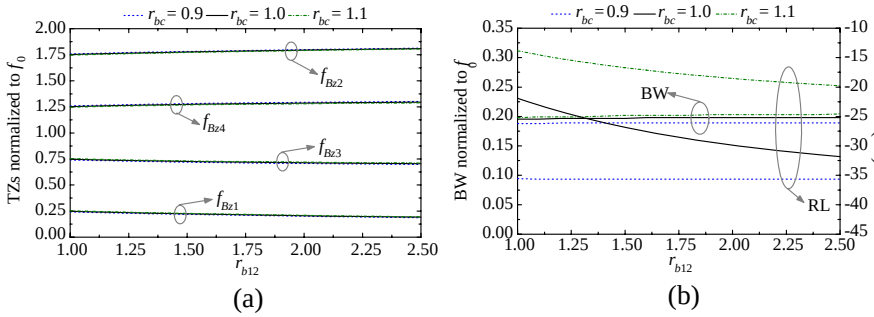

Figure 5. (a) Variation of TZs versus r_{bc} and r_{b12}. (b) Variation of BW and RL versus r_{bc} and r_{b12}.

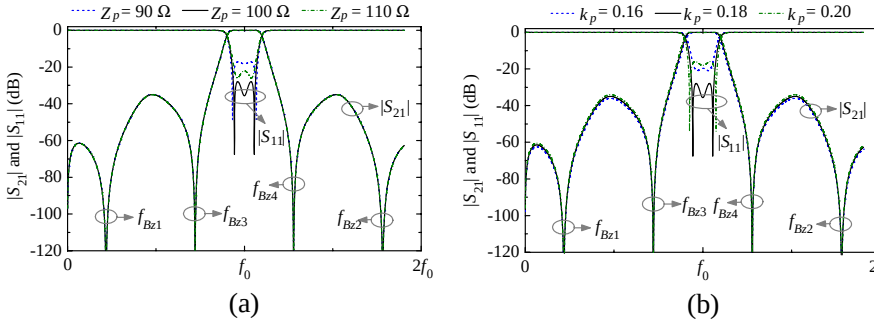

Figure 6. (a) Variation of $|S_{21}|$ and $|S_{11}|$ versus Z_p ($k_p = 0.18$ fixed). (b) Variation of $|S_{21}|$ and $|S_{11}|$ versus k_p ($Z_p = 100\,\Omega$ fixed).

can be mainly tuned by r_{bc} and k_c, and can be slightly tuned by k_p. The TZs of Filter B can be mainly tuned by r_{b12}. Lastly, the RL of Filter B can be achieved by tuning Z_p.

3.3. Filter *C*

For the BPF based on the anti-parallel coupled-line with Load C (named Filter C), $Z_{c1} = 110\,\Omega$ is firstly pre-selected. $k_c = 0.35$ is also pre-selected, because k_c has a weak effect on the TZs and can be used to tune BW, according to the above discussion. Under $Z_p = 100\,\Omega$ and $k_p = 0.21$, Figure 7 plots the variation of TZs, -3 dB BW and RL versus different values of $r_{cc} = Z_c/Z_{c1}$ and $r_{c12} = Z_{c2}/Z_{c1}$. It can be seen from Figure 7(a) that f_{Cz1} and f_{Cz2} of Filter C move close to f_0 as r_{b12} increases, while f_{Cz3} and f_{Cz4} of Filter C move apart from f_0 as r_{b12} increases. Figure 7(a) also shows that r_{cc} has a weak effect on

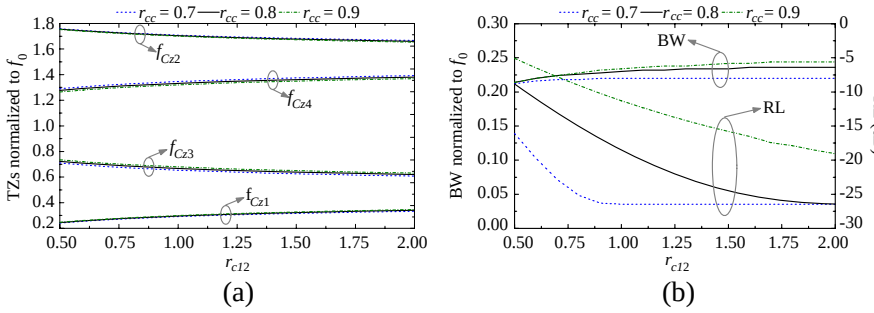

Figure 7. (a) Variation of TZs versus r_{cc} and r_{c12}. (b) Variation of BW and RL versus r_{cc} and r_{c12}.

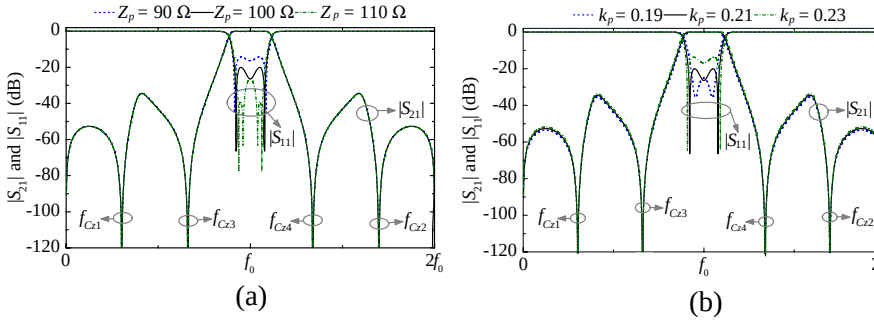

Figure 8. (a) Variation of $|S_{21}|$ and $|S_{11}|$ versus Z_p ($k_p = 0.21$ fixed). (b) Variation of $|S_{21}|$ and $|S_{11}|$ versus k_p ($Z_p = 100\,\Omega$ fixed).

f_{Cz1} and f_{Cz2}, but f_{Cz3} and f_{Cz4} move close to f_0 as r_{cc} increases. It can be seen from Figure 7(b) that -3 dB BW of Filter C increases as r_{cc} and r_{c12} increase. Figure 5(b) also shows that RL of Filter C becomes better as r_{c12} increases, and a smaller value of r_{cc} leads to a better RL. Under $r_{cc} = 0.8$ and $r_{c12} = 1.4$, Figure 8 plots the variation of $|S_{21}|$ and $|S_{11}|$ versus different values of Z_p and k_p. It can be seen from Figure 8(a) that Z_p can be used to tune $|S_{11}|$ separately and has almost no effect on BW. -3 dB BW of Filter C can be slightly tuned by k_p. Thus, -3 dB FBW of Filter C can be mainly tuned by r_{cc} and r_{c12}, and can be slightly tuned by k_p. The TZs of Filter B can be mainly tuned by r_{c12}. Lastly, the RL of Filter C can be achieved by tuning Z_p.

Table 1. Electrical specifications of designed BPFs.

	f_0 (GHz)	FBW	TZs (GHz)
Filter A	1.575	25%	0.823/2.327
Filter B	1.575	20%	0.342/1.145/2.005/2.808
Filter C	1.575	25%	0.476/1.055/2.095/2.674

Table 2. Designing parameters of proposed BPFs.

	Z_p (Ω)	k_p	Z_c (Ω)	k_c	Z_a (Ω)	Z_{b1} (Ω)	Z_{b2} (Ω)	Z_{c1} (Ω)	Z_{c2} (Ω)
Filter A	100	0.2	115	0.31	95	-	-	-	-
Filter B	99	0.18	87	0.3	-	87	140	-	-
Filter C	100	0.21	96	0.35	-	-	-	111	118

4. SIMULATED AND MEASURED RESULTS OF PROPOSED QUASI-ELLIPTIC WIDEBAND BANDPASS FILTERS (BPFS)

On the basis of the above discussion, three wideband BPFs with quasi-elliptic frequency response, i.e., Filter A, Filter B and Filter C, are designed, fabricated and measured. The electrical specifications of designed BPFs are tabulated in Table 1. Then, the designing parameter of these three BPFs are optimized as shown in Table 2. Three BPFs are designed on the substrate Arlon DiClad 880 ($h = 0.508\,\text{mm}$, $\varepsilon_{re} = 2.2$, $\tan\delta = 0.0009$). Figure 9(a), Figure 11(a) and Figure 13(a) give the layout of fabricated Filter A, Filter B and Filter C, respectively. After the initial physical dimensions are acquired with the help of ADS LineCalc tool, the whole structures are optimized in full-wave EM-simulator HFSS. The optimized physical dimensions of Filter A, Filter B and Filter C are also labeled in Figure 9(a), Figure 11(a) and Figure 13(a), respectively. Figure 9(b), Figure 11(b) and Figure 13(b) show photographs of fabricated Filter A, Filter B and Filter C, respectively. The overall circuit sizes of Filter A, Filter B and Filter C (not including the feeding lines) are $109\,\text{mm} \times 6.44\,\text{mm}$, $111.31\,\text{mm} \times 11.38\,\text{mm}$, $109.98\,\text{mm} \times 8.84\,\text{mm}$ respectively. Figure 10, Figure 12 and Figure 14 plot the simulated and measured results of fabricated Filter A, Filter B and Filter C, respectively. Good agreements between the simulations and measurements can be observed, and there are some

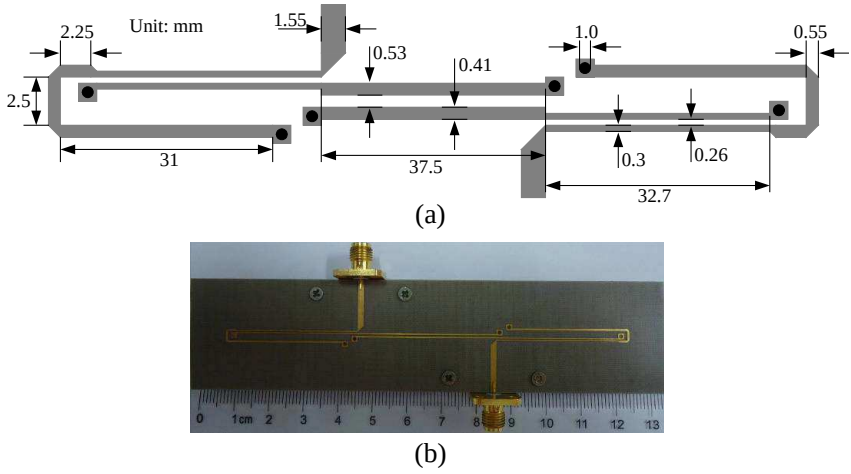

Figure 9. (a) Layout and (b) photograph of fabricated Filter A.

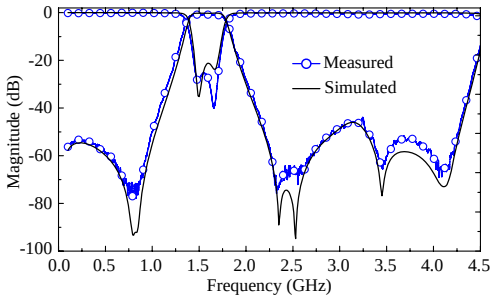

Figure 10. Simulated and measured S-parameters of the fabricated Filter A.

Table 3. Simulated and measured results of fabricated BPFs.

	Simulated				Measured			
	CF (GHz)/ FBW	IL at CF (dB)	RL (dB)	ROR (dB/GHz)	CF (GHz)/ FBW	IL at CF (dB)	RL (dB)	ROR (dB/GHz)
Filter A	1.585/24.6%	0.18	>20	124	1.59/25.1%	0.19	>26	129
Filter B	1.575/20.9%	0.3	>19	187.5	1.57/21.5%	1.12	>18	179
Filter C	1.585/23.3%	0.21	>21	165	1.58/23.1%	0.99	>19	164

slight discrepancies which are attribute to the fabrication error as well as SMA connectors. The simulated and measured central frequencies (CFs), insertion loss (IL), return loss (RL) and roll-off rate (ROR) are tabulated in Table 3.

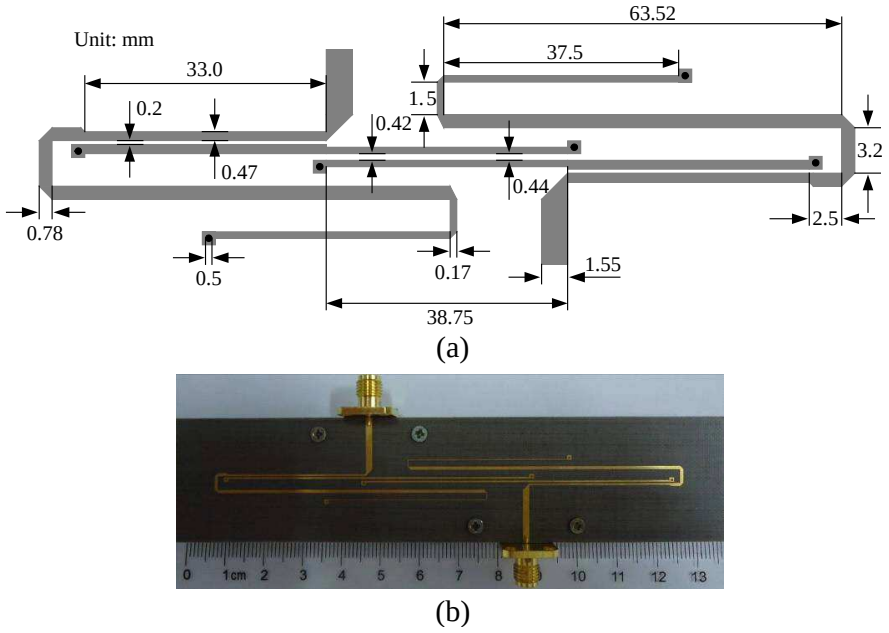

Figure 11. (a) Layout and (b) photograph of fabricated Filter B.

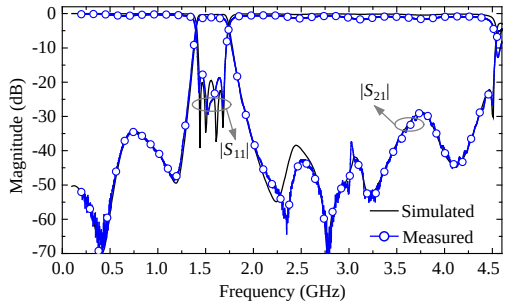

Figure 12. Simulated and measured S-parameters of the fabricated Filter B.

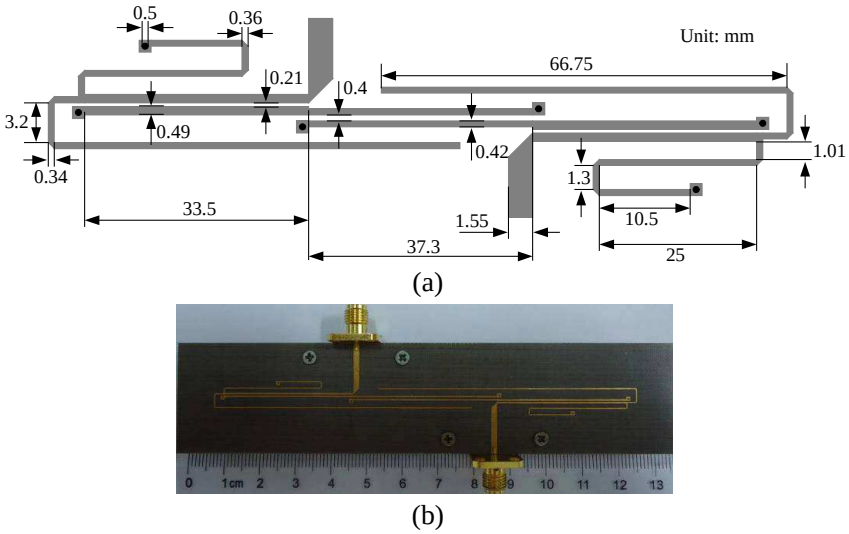

Figure 13. (a) Layout and (b) photograph of fabricated Filter C.

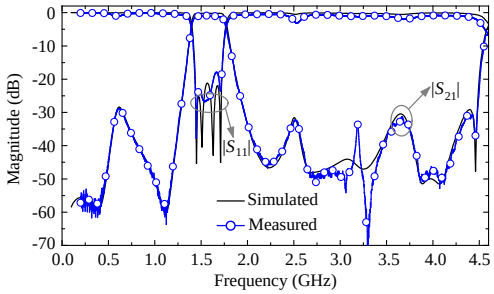

Figure 14. Simulated and measured S-parameters of the fabricated Filter C.

5. CONCLUSION

Three microstrip quasi-elliptic function bandpass filters based on the proposed stubs-loaded anti-parallel coupled-lines are presented in this paper. The proposed stubs-loaded anti-parallel coupled-lines have symmetrical transmission zeros along the designing frequency, and can improve the passband selectivity significantly when they are severed as input/output stages in bandpass filters. As examples, three bandpass filters centered at 1.575 GHz have been successfully demonstrated. Results indicate that the demonstrators have the properties of low

in-band insertion loss, good in-band return loss, sharp passband selectivity and high out-of-band rejection. With all these good features, the proposed filters are applicable to modern communication systems.

REFERENCES

1. Wu, Y., Y. Liu, S. Li, and C. Yu, "A new wide-stopband lowpass filter with generalized coupled-line circuit and analytical theory," *Progress In Electromagnetics Research*, Vol. 116, 553–567, 2011.
2. Wu, Y. and Y. Liu, "A coupled-line bandstop filter with three-section transmission-line stubs and wide upper passband performance," *Progress In Electromagnetics Research*, Vol. 119, 407–421, 2011.
3. Cui, D., Y. Liu, Y. Wu, S. Li, and C. Yu, "A compact bandstop filter based on two-meandered parallel-coupled lines," *Progress In Electromagnetics Research*, Vol. 121, 271–279, 2011.
4. Liu, G. and Y. Wu, "Novel in-line microstrip coupled-line bandstop filter with sharp skirt selectivity," *Progress In Electromagnetics Research*, Vol. 137, 585–597, 2013.
5. Cheong, P., S.-W. Fok, and K.-W. Tam, "Miniaturized parallel coupled-line bandpass filter with spurious-response suppression," *IEEE Trans. Microw. Theory Tech.*, Vol. 53, No. 5, 1810–1816, 2005.
6. Lee, S. and Y. Lee, "Generalized miniaturization method for coupled-line bandpass filters by reactive loading," *IEEE Trans. Microw. Theory Tech.*, Vol. 58, No. 9, 2383–2391, 2010.
7. Park, J.-H., S. Lee, and Y. Lee, "Extremely miniaturized bandpass filters based on asymmetric coupled lines with equal reactance," *IEEE Trans. Microw. Theory Tech.*, Vol. 60, No. 2, 261–269, 2012.
8. Tiwary, A. K. and N. Gupta, "Design of compact coupled microstrip line bandpass filter with improved stopband characteristics," *Progress In Electromagnetics Research C*, Vol. 24, 97–109, 2011.
9. Hua, C., C. Chen, C. Miao, and W. Wu, "Microstrip bandpass filters using dual-mode resonators with internal coupled lines," *Progress In Electromagnetics Research C*, Vol. 21, 99–111, 2011.
10. Wu, C.-H., Y.-S. Lin, C.-H. Wang, and C. H. Chen, "Compact microstrip coupled-line bandpass filter with four transmission zeros," *IEEE Microw. Wireless Compon. Lett.*, Vol. 15, No. 9, 579–581, 2005.
11. Wong, S. W., K. Wang, Z. N. Chen, and Q. X. Chu, "Rotationally

symmetric coupled-lines bandpass filter with two transmission zeros," *Progress In Electromagnetics Research*, Vol. 135, 641–656, 2013.

12. Wang, L. and L. Jin, "A quasi-elliptic microstrip bandpass filter using modified anti-parallel coupled-line," *Progress In Electromagnetics Research*, Vol. 138, 245–253, 2013.
13. Miller, A. and J.-S. Hong, "Reconfigurable cascaded coupled line filter with four distinct bandwidth states," *IET Microw. Antennas Propag.*, Vol. 5, No. 14, 1730–1737, 2011.
14. Marimuthu, J., A. M. Abbosh, and B. Henin, "Planar microstrip bandpass filter with wide dual bands using parallel-coupled lines and stepped impedance resonators," *Progress In Electromagnetics Research C*, Vol. 35, 49–61, 2013.
15. Kuo, J. T., C.-Y. Fan, and S.-C. Tang, "Dual-wideband bandpass filters with extended stopband based on coupled-line and coupled three-line resonators," *Progress In Electromagnetics Research*, Vol. 124, 1–15, 2012.
16. Lee, S. and Y. Lee, "A planar dual-band filter based on reduced-length parallel coupled lines," *IEEE Microw. Wireless Compon. Lett.*, Vol. 20, No. 1, 16–18, 2010.
17. Lee, S. and Y. Lee, "A uniform coupled-line dual-band filter with different bandwidths," *IEEE Microw. Wireless Compon. Lett.*, Vol. 20, No. 10, 545–547, 2010.
18. George, I. Z. and A. K. Johnson, "Coupled transmission line networks in an inhomogeneous dielectric medium," *IEEE Trans. Microw. Theory Tech.*, Vol. 17, No. 10, 753–759, 1969.
19. Hong, J. S. and M. J. Lancaster, *Microstrip Filter for RF/Microwave Applications*, Wiley, New York, 2001.